

## Performance of Helical Magnets for RHIC\*

Erich Willen, Michael Anerella, John Escallier, George Ganetis, Arup Ghosh, Animesh Jain, Eugene Kelly, Gerry Morgan, Joseph Muratore, Albert Prodell, Peter Wanderer  
Brookhaven National Laboratory, Upton, NY

Ramesh Gupta  
Lawrence Berkeley National Laboratory, Berkeley, CA

Masahiro Okamura  
RIKEN, Japan

**Abstract**—Helical magnets are being built for the Relativistic Heavy Ion Collider (RHIC) to act as Snakes and Rotators in a planned program of polarized colliding beam experiments. After a successful R&D program, production is underway to build the needed magnets. They are constructed as superconducting, 10 cm coil aperture units in which a 4 T dipole field rotates through 360 degrees in a length of 2.4 m. Measurements have been made on the initial production magnets, including training, magnetic fields, and quench propagation characteristics.

### I. INTRODUCTION

Previous papers [1-5] have described the techniques that will be used to control the spin of protons in RHIC and have given design considerations for the helical magnets being built to provide the required magnetic fields. A recent paper [6] gave construction details of these magnets. Another recent paper [7] summarizes the field requirements and construction details, and gives some measurement results for the magnets. Measurements are now complete on the initial four, 4 T, 2.4 m long magnets that constitute a complete Snake. Results presented here include the quench performance of the four magnets, their magnetic field quality, and the quench propagation characteristics as studied in one specially instrumented magnet.

### II. DESIGN

The magnets are 100 mm aperture dipoles built by placing small diameter superconducting cable into helical slots milled into thick-walled aluminum cylinders. The coils were designed with a 2D program and the design of the magnet including the iron yoke was checked with a detailed 3D analysis of the field [5]. An iron yoke is placed around these coils and the entire structure constitutes one 2.4 m long magnet in which the dipole field rotates through 360° over

this length. A cylindrical shell is welded around four of these magnets. This assembly is placed into a cryostat to make a Snake or a Rotator.

The particular field that is powered in each magnet, its angular orientation and its helicity determine whether the unit will act as a Snake or a Rotator in the RHIC lattice. There are 16 separate helical slots constituting 16 separate windings in one magnet. These windings are connected in series at the end of the magnet. A quench protection resistor made of nichrome wire is installed across each winding to dissipate the stored magnetic energy and to avoid dangerous voltages during a quench. A simple resistor across each winding can be tolerated because the magnet is not ramped or is ramped only slowly when beam is in the machine. The multiple current leads exiting the cold environment with the consequent high cryogenic load for the entire Snake/Rotator ensemble dictated the use of a low current design for the magnet. Fig. 1 shows a cross section view of the magnet design. Fig. 2 is a photograph of a section cut from the earlier prototype magnet. Table I lists a few relevant parameters.

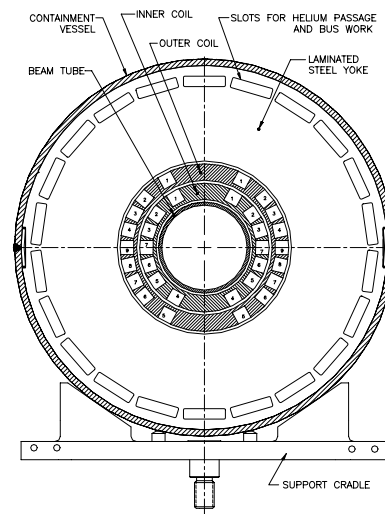


Fig. 1. Cross section of the helical magnet. The yoke diameter is 355.6 mm. The conductor inner diameter is 100 mm. The coil tube outer diameters are 125.6 mm, 163.2 mm.

\* Work supported by RIKEN and the US Department of Energy

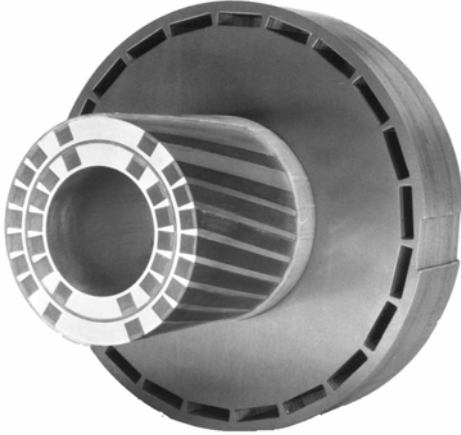


Fig. 2. Photograph of a section cut from the prototype helical magnet.

TABLE I

SELECTED PARAMETERS OF THE HELICAL MAGNET.

Parameter	Units	Value
Aperture	mm	100
Magnetic length	m	2.4
Field	T	4
Current	A	320
Number of turns		1680
Inductance	H	4.8
Stored energy @ 4 T	kJ	240
Diameter of yoke	mm	355.6
Num. of strands in cable		7
Strand diameter	mm	0.33
Cu to non-Cu ratio		2.5:1

### III. QUENCH PERFORMANCE

For cryogenic testing, each magnet is suspended vertically in a dewar filled with liquid helium at 1.3 atm pressure, 4.5 K temperature. The magnet current is ramped up until a quench is detected in the magnet. This training process is repeated until the short sample limit of the conductor is reached or until a satisfactorily high current in the magnet is achieved. The quench performance for the four magnets in the first Snake is shown in Fig. 3. Some training is required but each magnet achieved a suitable current in a reasonable number of steps. The quench level achieved is found to be retained in a thermal cycle of the magnet.

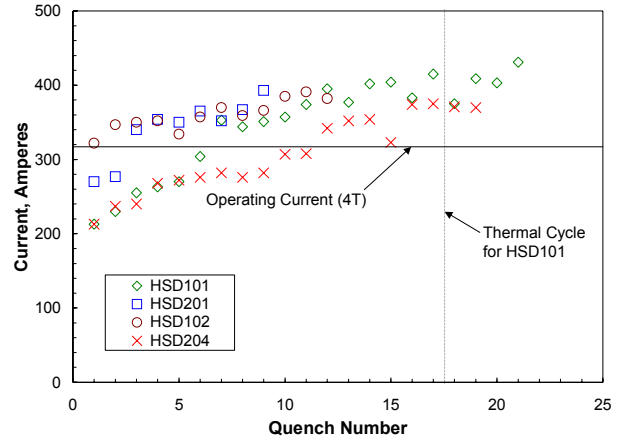


Fig. 3. Quench performance of the four magnets of the first Snake. After some initial training, each reached a current comfortably above the maximum operating point of 4 T. A thermal cycle showed no retraining.

### IV. DESCRIPTION OF THE FIELD

For a helical dipole magnet, the transverse magnetic field components in cylindrical coordinates may be expanded in terms of multiple coefficients  $\tilde{b}_n$  and  $\tilde{a}_n$  as

$$B_r(r, \tilde{\theta}) = B_0 \sum_{n=0}^{\infty} \left[ \frac{2^{n+1}(n+1)!}{(n+1)^{n+1} (kR_{ref})^n} \right] I'_{n+1}((n+1)kr) \times [\tilde{b}_n \sin((n+1)\tilde{\theta}) + \tilde{a}_n \cos((n+1)\tilde{\theta})]$$

$$B_\theta(r, \tilde{\theta}) = B_0 \sum_{n=0}^{\infty} \left[ \frac{2^{n+1}(n+1)!}{(n+1)^{n+1} (kR_{ref})^n} \right] \frac{I_{n+1}((n+1)kr)}{kr} \times [\tilde{b}_n \cos((n+1)\tilde{\theta}) - \tilde{a}_n \sin((n+1)\tilde{\theta})]$$

$$B_z(r, \tilde{\theta}) = -(kr)B_\theta(r, \tilde{\theta}).$$

Here,  $B_0$  is the dipole field,  $n=1$  refers to the quadrupole term,  $I_n$  is the modified Bessel function,  $k = d\alpha/dz$  is the rate of change of the dipole field angle,  $R_{ref}$  is the reference radius, and  $\tilde{\theta} = \theta - kz$ . The coordinate  $z$  is measured along the axis and  $\theta$  is the polar angle relative to the horizontal plane. The tilda on the multipole coefficients  $\tilde{b}_n$ ,  $\tilde{a}_n$  indicates that these coefficients are with reference to the changing field angle along the length of the magnet.

A helical field expressed in Cartesian coordinates,  $B_x, B_y$ , contains components that are non-linear in  $x, y$ , even with only  $n=0$  terms in  $B_r$  and  $B_\theta$  [7]. Measurements made with a rotating coil in such a field, described below, do not

measure these components directly as e.g. sextupole, though the total field as expressed above is correctly measured.

## V. MAGNETIC FIELD MEASUREMENTS

### A. Integral Field

The integral field of a magnet is measured using a 3.57 m long, 48 mm diameter rotating coil with tangential windings on its cylindrical surface. The voltage induced in this coil is measured at various fixed currents. In principle, the field measured in this way should be zero, though both construction errors in the magnet and in the measuring coil could give a non-zero value. The tolerance specified for a helical magnet is

$$\left[ \left( \int B_y(z) dz \right)^2 + \left( \int B_x(z) dz \right)^2 \right]^{1/2} < 5 \times 10^{-2} \text{ T} \cdot \text{m}.$$

This tolerance in terms of rotation angle is  $\sim 1.9$  degrees.

An analysis of the effect of measuring coil construction errors on the integral field measurement has been performed [8]. In this analysis, the coil was divided into a number of sections, random radius and angular position errors assigned to each section, and the measurement error calculated if the coil were measuring a perfect magnet. The distribution of errors for repeated such calculations gave a mean of  $0.370^\circ$  and a standard deviation of  $0.179^\circ$ . Therefore, the effect of measuring coil construction errors on an integral field measurement is well within the required tolerance on a magnet.

The integral field measurement on magnet HSD102 is shown in Fig. 4. For the four magnets in the Snake, the mean of such measurements, taking the maximum measured value for each measurement, was found to be  $0.0170 \text{ T} \cdot \text{m}$  and the standard deviation  $0.0038 \text{ T} \cdot \text{m}$ , both safely within the specification value of  $0.0500 \text{ T} \cdot \text{m}$ .

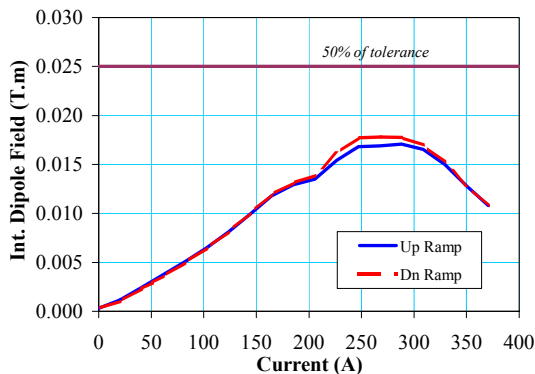


Fig. 4. The integral field measured in magnet HSD102.

### B. Field Including Harmonics

The field in each magnet is measured with a 51 mm long, 68 mm diameter tangential coil. Because the field rotates over the length of these straight windings, the measurement has a small error that varies with harmonic number. A correction, derived in a separate calculation, is applied to the data in the analysis; for the dipole, the measurement is low by a factor of 0.9992, for the sextupole 0.9932, for the decapole 0.9811, for the 14-pole 0.9632.

1) *Field vs. Current at Center of Magnet:* The field was measured as a function of current at the center of the magnet. Plots of typical measurements, in magnet HSD201 at the center of the magnet, are shown in the Figs. 5 to 8. “Units” are defined as parts in  $10^{-4}$  of the dipole field. The quadrupole component (Fig. 6) is believed to be caused by a distortion of the cylindrical coil tubes. The decrease in the transfer function (Fig. 5) and the increasing sextupole component (Fig. 7) with current are caused by saturation of the steel yoke, which is intentionally undersized in order to limit the physical size of the magnet.

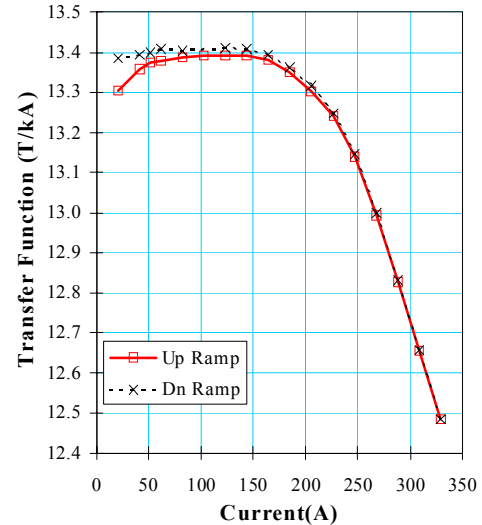


Fig. 5. Typical transfer function, measured in magnet HSD201 at the center of the magnet.

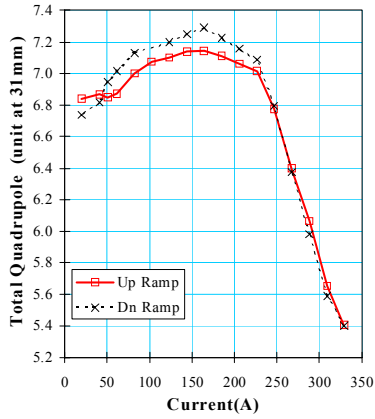


Fig. 6. Quadrupole component measured in magnet HSD201 at the center of the magnet.

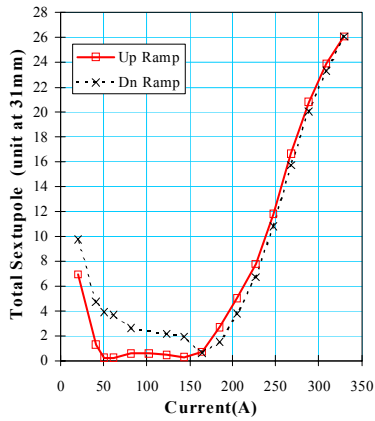


Fig. 7. Sextupole component measured in magnet HSD201 at the center of the magnet.

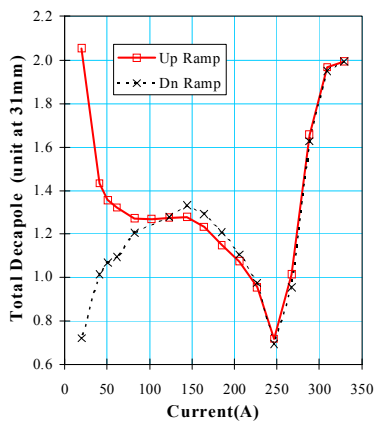


Fig. 8. Decapole component measured in magnet HSD201 at the center of the magnet.

2) *Field vs. Position on Magnet Axis:* The field was measured as a function of axial position at three currents (fields): 102 A (1.37 T); 267 A (3.47 T); and 329 A (4.11 T).

Plots of the measurements in magnet HSD102 are shown in Figs. 9 to 13.

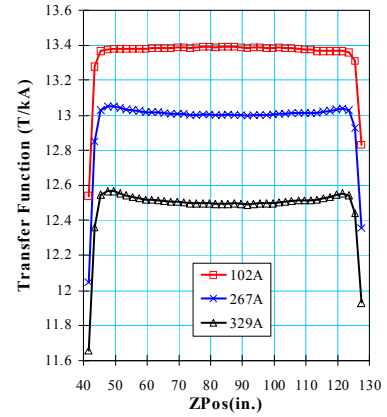


Fig. 9. The transfer function in magnet HSD102 measured along the length of the magnet.

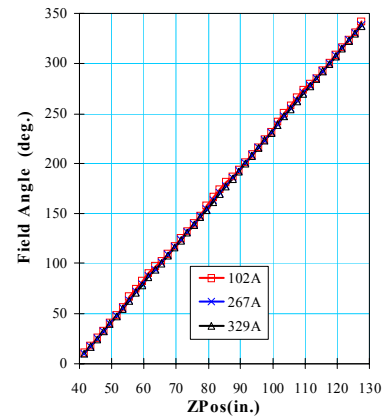


Fig. 10. The dipole field angle in magnet HSD102 measured along the length of the magnet.

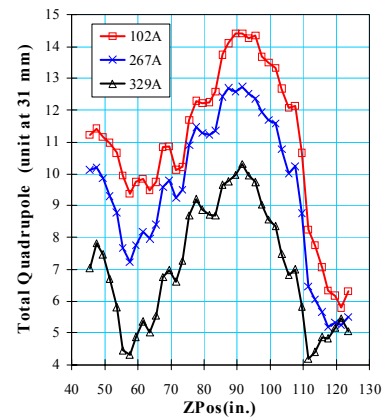


Fig. 11. The quadrupole field component in magnet HSD102 measured along the length of the magnet.

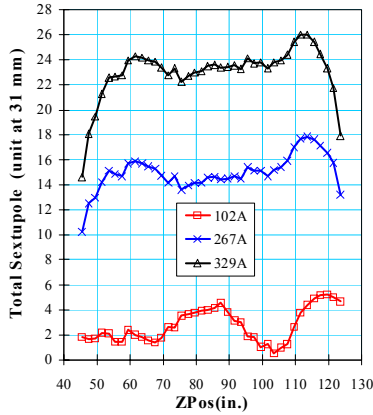


Fig. 12. The sextupole field component in magnet HSD102 measured along the length of the magnet. Saturation of the steel yoke is responsible for the increase at high current.

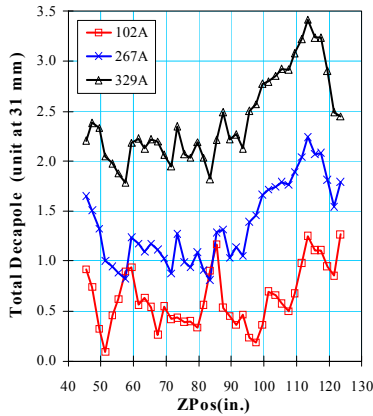


Fig. 13. The decapole field component in magnet HSD102 measured along the length of the magnet.

3) *Tables of Field Harmonics:* Tables II and III summarize the field harmonics measured in the straight sections of the four magnets comprising the first Snake. For each magnet, the number used in the table is actually the average for measurements made in 51 mm steps over the uniform field between the ends, some 30 steps in all.

## VI. QUENCH PROTECTION

Each of the 16 windings of the helical magnet is protected with a 50 mΩ bypass resistor wired across the winding. As a quench develops in a particular winding, its resistance builds and the magnet current passes increasingly through the bypass resistor, thereby reducing the energy that would otherwise be dissipated in the winding. The stored magnetic energy in the winding that quenches, however, is mostly absorbed by the winding itself.

It had been observed in the quench testing of the magnets,

TABLE II

NORMAL HARMONICS IN THE FOUR MAGNETS OF THE FIRST SNAKE. RESULTS ARE GIVEN IN UNITS OF  $10^{-4}$  OF THE DIPOLE FIELD AT A REFERENCE RADIUS OF 31 MM.

Harmonic	Mean @102A	Mean @329A	Std. Dev. @102A	Std. Dev. @329A
$\tilde{b}_1$ (quad)	-1.32	-0.65	3.24	2.26
$\tilde{b}_2$	-1.84	-25.42	3.02	3.90
$\tilde{b}_3$	0.15	0.13	0.45	0.46
$\tilde{b}_4$	0.71	-1.71	0.83	0.76
$\tilde{b}_5$	0.01	0.00	0.17	0.19
$\tilde{b}_6$	0.19	0.75	0.22	0.25
$\tilde{b}_7$	-0.02	-0.02	0.01	0.01
$\tilde{b}_8$	-7.84	-8.64	0.27	0.28

TABLE III

SKREW HARMONICS IN THE FOUR MAGNETS OF THE FIRST SNAKE. RESULTS ARE GIVEN IN UNITS OF  $10^{-4}$  OF THE DIPOLE FIELD AT A REFERENCE RADIUS OF 31 MM.

Harmonic	Mean @102A	Mean @329A	Std. Dev. @102A	Std. Dev. @329A
$\tilde{a}_1$ (quad)	0.20	-0.22	4.85	4.12
$\tilde{a}_2$	0.81	0.84	0.36	0.32
$\tilde{a}_3$	0.52	0.64	0.86	1.02
$\tilde{a}_4$	0.15	0.12	0.17	0.21
$\tilde{a}_5$	-0.30	-0.31	0.56	0.61
$\tilde{a}_6$	-0.01	-0.04	0.12	0.14
$\tilde{a}_7$	0.01	0.01	0.03	0.03
$\tilde{a}_8$	0.09	0.10	0.08	0.08

where voltage taps are routinely placed across each winding in order to identify the winding that quenches, that natural quenches at all currents spread quickly through the other windings of the magnet, induced there by coupling through the large mutual inductance of the windings. However, the temperature reached at the quench origin can not be

determined from these routine measurements. Therefore, magnet HSD102 was instrumented to study the quenching process in detail. Redundant spot heaters and local voltage taps were applied to the pole winding of the outer coil in the straight section and at the very end of its mid-plane winding. Leads that could be used to measure the current through the bypass resistor of the designated winding during a quench were brought to the outside of the test dewar. The difference between this current and the total current then represented the current through the winding in which a quench was triggered with the spot heater.

The voltage measured with the local voltage taps was used to calculate the resistance of the quenching section of the windings. Using the known resistance vs. temperature characteristic of the conductor, the maximum temperature was inferred for a variety of quenching conditions.

It was found that the temperatures reached during quenches in the straight section of the pole winding were quite low—the maximum recorded was 80 K at the maximum measured current, 380 A. Quenches below 300 A developed temperatures less than 50 K. At the end of the mid-plane winding, however, the temperature reached 590 K for a current of 365 A. While still below the burnout temperature of ~800 K, this is uncomfortably high. Fortunately, the magnet is not expected to quench spontaneously in that location because of the ample operating margin of the conductor there.

## VII. CONCLUSIONS

The quench performance of the magnets, after some training, is suitable for machine use. The integral field is well within

tolerable limits. Field harmonics are not critical in this application and are acceptable as measured. The quench protection studies show that the magnets with a quench protection resistor across each winding are safe against damage from spontaneous quenches in operation.

## REFERENCES

- [1] E. Willen, R. Gupta, A. Jain, E. Kelly, G. Morgan, J. Muratore, R. Thomas, "A helical magnet design for RHIC," *Proc. PAC97*, Vancouver, BC, p. 3362, May, 1997.
- [2] M. Syphers et al., "Helical dipole magnets for polarized protons in RHIC," *ibid.*, p. 3359.
- [3] *Design Manual: Polarized Proton Collider at RHIC*, M. Syphers, Editor, BNL, July, 1998.
- [4] M. Okamura, T. Tominaka, T. Kawaguchi, A. Jain, R. Thomas, E. Willen, "Field calculations and measurements of a helical Snake magnet for RHIC," *Proc. MT15*, Beijing, October, 1997, published by Science Press, Beijing, p. 250.
- [5] T. Katayama, et al., "Field calculation and measurement of a full length Snake magnet for RHIC," *Proc. EPAC*, Stockholm, June, 1998.
- [6] E. Willen, et al., "Construction of helical magnets for RHIC," *Proc. PAC99*, New York, March-April, 1999.
- [7] W. MacKay, et al., "Superconducting helical Snake magnets: construction and measurements," *Proc. Workshop on Polarized Protons at High Energies*, Hamburg, May, 1999; *BNL Spin Note 80*, August, 1999.
- [8] A. Jain, "Measurement of integral field of helical dipoles," *Proc. 11th International Magnet Measurement Workshop*, BNL, September, 1999.